



EFFECT OF Au PLASMONIC NANOPARTICLES ON SHORT-CIRCUIT CURRENT DENSITY OF PbS QUANTUM DOT SENSITIZED SOLAR CELLS

T. Jaseetharan^{1,2}, W.I. Sandamali^{2,3}, G.K.R. Senadeera^{2,3}, V.P.S. Perera³, J.C.N. Rajendra³, N. Karthikeyan³, Lahiru A. Wijenayaka⁴, M.A.K.L. Dissanayake²*

¹*Department of Physical Sciences, South Eastern University of Sri Lanka, Sri Lanka*

²*National Institute of Fundamental Studies, Sri Lanka*

³*Department of Physics, The Open University of Sri Lanka, Sri Lanka*

⁴*Department of Chemistry, The Open University of Sri Lanka, Sri Lanka*

INTRODUCTION

Quantum dots are the sensitizers in quantum dot-sensitized solar cells (QDSSCs) and they absorb photons and generate electron-hole pairs. For efficient electron injection, the conduction band edge of the quantum dot should be higher than the conduction band of the electron transporting material (TiO₂) in the photoanode. However, the energy gaps of the quantum dot can be changed by quantum confinement effects for solar cell applications (Eskandari et al., 2015). In order to produce a high photocurrent, quantum dots should absorb the photons from a wide range of solar spectrum and should have a high absorption coefficient.

QDSSC mainly consists of photoanode, electrolyte and counter electrode. Photoanode is fabricated through the deposition of mesoporous semiconductor material on conducting glass substrate and sensitized with quantum dots. Electrolyte contains a redox couple which is filled between the photoanode and counter electrode. Counter electrode is used for the charge exchange. Upon illumination, quantum dot is excited to a higher energy state and excitons are created. Due to the band alignment, excited electrons are injected to the conduction band of the TiO₂ and the holes are scavenged by the electrolyte. Electrons diffuse through the mesoporous TiO₂ and reach the conducting glass substrate (FTO glass) and enter the external load performing work. Finally, these electrons reach the counter electrode and regenerate the oxidized component of the redox couple in the electrolyte. Performance of QDSSC can be enhanced by modifying the counter electrode, photoanode and the electrolyte.

In the present study, TiO₂ nanoparticle photoanode based PbS QDSSCs have been fabricated with suitable SILAR cycles. In order to enhance the performance of the QDSSCs, different amounts of colloidal Au plasmonic nanoparticles were added to the TiO₂ photoanode.

METHODOLOGY

Synthesis of Au colloidal nanoparticles

Au nanoparticle solution was prepared using the citrate reduction method (Kumar et al., 2012). 0.1 g of trisodium citrate (Na₃C₆H₅O₇) was dissolved in 10 ml of deionized water and 1 mM of tetrachloroauric acid (HAuCl₄) solution was prepared with 20 ml deionized water. This solution was boiled under continuous stirring and 2 ml of Na₃C₆H₅O₇ solution was added to the boiling HAuCl₄ solution. When the colour of the mixture became deep red, the hotplate was turned off and the solution was allowed to cool.

Preparation of TiO₂ electrodes

0.25 g of TiO₂ P90 powder was ground well for 15 minutes with 1 ml of 0.1 M HNO₃. The paste was spin coated on the conducting side of FTO glass at 3000 rpm for 1 minute and sintered at 450 °C for 45 minutes. For preparation of TiO₂ P25 paste, 0.25 g of TiO₂ powder and 1 ml of 0.1 M HNO₃ were ground using mortar and pestle. Then, 0.02 g of Triton X-100 and 0.05 g of Poly ethylene glycol 1000 were used as the binder and the mixture was ground until it became a creamy paste (Kumari et al., 2017). In order to study the plasmonic effect, different amounts of Au nanoparticle colloidal were added and the paste was ground for another 15 minutes to get a



homogeneous distribution of Au nanoparticles in the TiO₂ P25 paste. The TiO₂ P25 nanoparticle paste containing Au nanoparticles were spin coated on TiO₂ P90 layer at 1000 rpm for 1 minute. Finally, the electrodes were sintered for 45 minutes at 450 °C. The structure of the electrode is FTO/TiO₂ P90/(TiO₂ P25 + Au nanoparticles).

Deposition of quantum dots

PbS quantum dots were deposited on TiO₂ electrodes by the successive ionic layer adsorption and reaction (SILAR) method. Aqueous solutions of 0.1 M Pb(NO₃)₂ and 0.1 M Na₂S were used as cationic precursor solution and anionic precursor solution respectively. In this method, the electrode is immersed alternatively into cationic and anionic precursor solutions. Between immersing processes, the electrode was rinsed in deionized water and dried.

Preparation of polysulfide electrolyte

Polysulfide electrolyte was prepared by dissolving 2 M Na₂S and 2 M S in a mixture of water and methanol in the ratio of 3:7 (v/v). The mixture was subjected to magnetic stirring at room temperature until all the sulfur was dissolved.

Preparation of Cu₂S counter electrode

A cleaned brass plate was immersed in conc. HCl at 80 °C for 10 minutes. A scotch tape mask with appropriate area was applied on the surface of the treated brass plate. Synthesized polysulfide electrolyte was applied to the unmasked area which became black in colour due to the formation of Cu₂S. This electrode was used as the counter electrode of the QDSSCs.

Cell assembly and current-voltage characterization

An appropriate amount of polysulfide electrolyte was applied on the unmasked area of the Cu₂S counter electrode. Photoanode was placed on the electrolyte so that the active sides of both electrodes were facing each other with the electrolyte in between them and held together using steel clips. Current-voltage measurements of each QDSSCs were done under the illumination of 100 mW cm⁻² with AM 1.5 spectral filter using a computer controlled multi-meter (Keithley 2000 model) coupled with potentiostat/galvanostat unit (HA-301). The active area of the QDSSC was 0.12 cm².

Optical absorption measurements

Optical absorption spectra of colloidal Au nanoparticles, TiO₂/Au NP electrode and TiO₂/Au NP/PbS were obtained using Shimadzu 2450 spectrophotometer in the wavelength range between 350 nm to 1100 nm.

Morphology analysis and EDX spectrum measurement

Morphology of the Au colloidal nanoparticles was examined by using JEOL JEM-2100 High resolution transmission electron microscope (HRTEM) with an accelerating voltage of 200 kV. Energy dispersive X-ray (EDX) spectrum was obtained by using Ametek EDAX module with Octane T Optima-60 EDX detector in TEM mode.

RESULTS AND DISCUSSION

Figure 1 shows the high-resolution TEM images of the Au colloidal nanoparticles. According to the HRTEM image, it can be seen that the sizes of the Au nanoparticles are in the range between 25 and 35 nm.

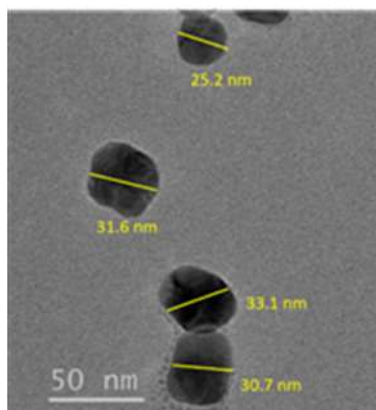


Figure 1: HRTEM image of Au colloidal nanoparticles

Figure 2 shows the optical absorption spectrum of plasmonic Au nanoparticles. It shows a broad absorption in the visible region which peaks around 527 nm. From this absorption maximum, the average particle size of the Au nanoparticles has been approximately estimated by comparing the published articles, which is in the range of 25-35 nm and the shape of the particles are nearly spherical (Link & El-Sayed, 1999). This result was confirmed with TEM images.

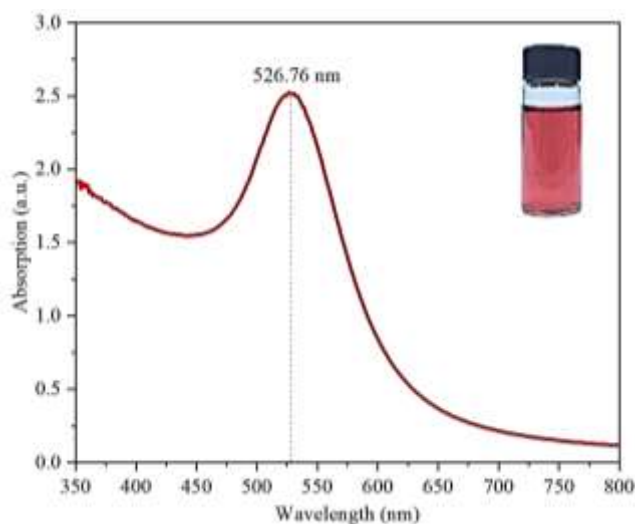


Figure 2: Optical absorption spectrum of colloidal Au nanoparticles

Figure 3 shows the optical absorption spectra of TiO_2 , TiO_2/Au and $\text{TiO}_2/\text{Au}/\text{PbS}$ electrodes. Au nanoparticle incorporated electrode shows a broad peak in the visible region between 500 nm and 550 nm. This peak clearly confirms the presence of Au plasmonic nanoparticles in the TiO_2 electrode. $\text{TiO}_2/\text{Au}/\text{PbS}$ photoanode shows a broad peak around 500-550 nm. Also, this photoanode exhibits another very strong absorption peak at around 1050 nm in the near IR region evidently due to the optical absorption by PbS Quantum dots (McDonald et al., 2005).

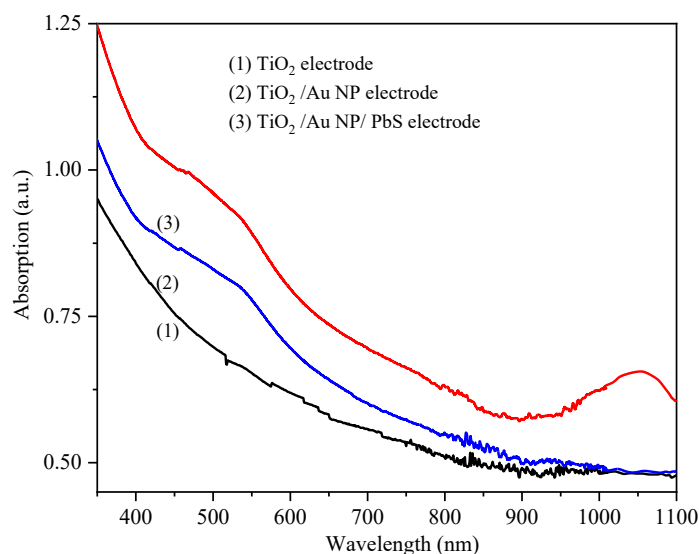


Figure 3: Optical absorption spectra of (1) TiO_2 electrode, (2) $\text{TiO}_2/\text{Au NP}$ electrode, and (3) $\text{TiO}_2/\text{Au NP}/\text{PbS}$ electrode

The EDX spectrum of $\text{TiO}_2/\text{Au}/\text{PbS}$ photoanode is shown in Figure 4. EDX spectrum confirms the existence of Au, Pb and S in the TiO_2 electrode.

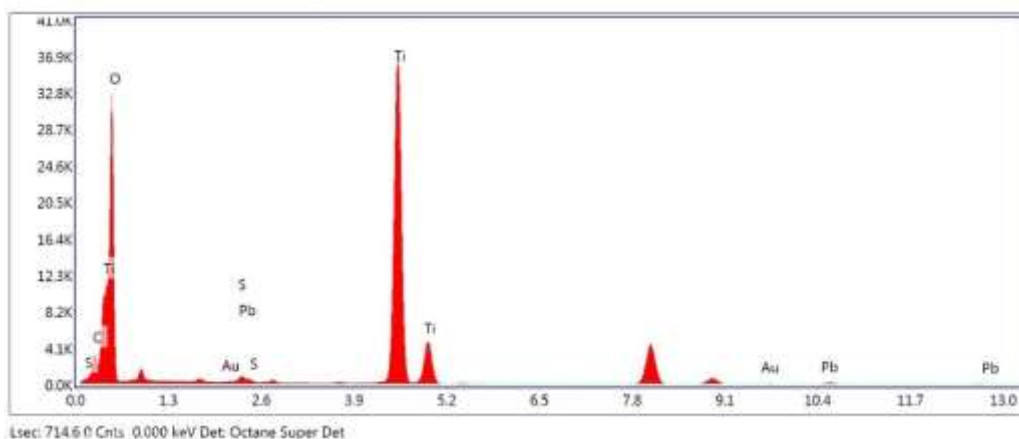


Figure 4: EDX spectrum of $\text{TiO}_2/\text{Au}/\text{PbS}$ photoanode

Figure 5 shows the current-voltage characterization of TiO_2/PbS photoanodes with and without Au nanoparticles under the simulated sunlight of 100 mW cm^{-2} with AM 1.5 spectral filter. Au nanoparticle incorporated PbS quantum dot-sensitized solar cells show improved photovoltaic performance compared to the controlled device. This is evidently due to the enhanced photocurrent in the quantum dot-sensitized solar cell with Au nanoparticles, compared to device without Au nanoparticles, under similar fabrication and light conditions caused by the localized surface plasmon resonance (LSPR) effect (Gonfa et al., 2016; Smith et al., 2015). Photovoltaic parameters are summarized in Table 1.

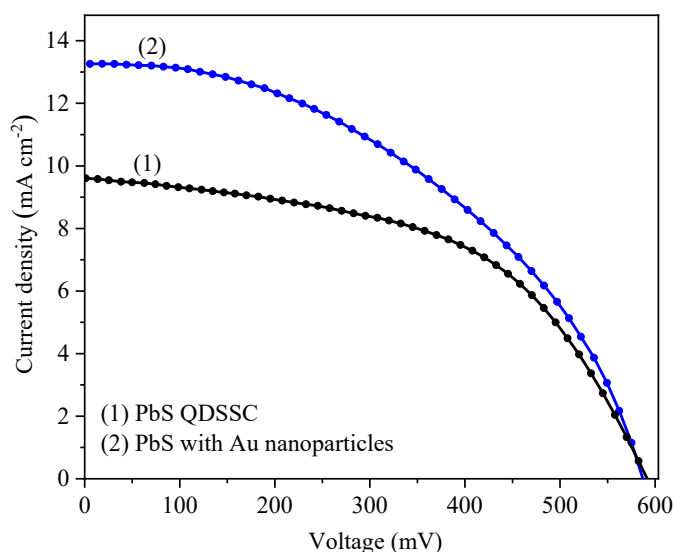


Figure 5: Current-voltage characterization of PbS QDSSCs with and without Au nanoparticles

Table 1: Photovoltaic parameters of PbS QDSSCs

TiO ₂ Photoanode	J_{sc} (mA cm ⁻²)	V_{oc} (mV)	FF (%)	Efficiency (%)
Without Au NPs	9.71	590.3	54.0	3.09
With Au NPs	13.12	586.7	55.2	4.24

CONCLUSIONS/RECOMMENDATIONS

Plasmonic gold nanoparticles were synthesized and characterized. PbS quantum dot-sensitized solar cells have been fabricated using TiO₂ electrodes. Au plasmonic nanoparticles have been incorporated into the TiO₂ electrode. PbS quantum dot-sensitized, plasmonic solar cells show a significantly higher efficiency of 4.24% compared to the control device (3.09%) without Au nanoparticles. This is evidently due to the enhanced photocurrent in the quantum dot-sensitized solar cell with Au nanoparticles, compared to a device without Au nanoparticles, under similar fabrication and light conditions caused by the localized surface plasmon resonance (LSPR) effect.

REFERENCES

- Eskandari, M., Ahmadi, V., Yousefi Rad, M., & Kohnepoushi, S. (2015). Plasmon enhanced CdS-quantum dot sensitized solar cell using ZnO nanorods array deposited with Ag nanoparticles as photoanode. *Physica E: Low-Dimensional Systems and Nanostructures*, 68, 202–209. <https://doi.org/10.1016/j.physe.2014.12.007>
- Gonfa, B. A., Kim, M. R., Zheng, P., Cushing, S., Qiao, Q., Wu, N., El Khakani, M. A., & Ma, D. (2016). Investigation of the plasmonic effect in air-processed PbS/CdS core-shell quantum dot based solar cells. *Journal of Materials Chemistry A*, 4(34), 13071–13080. <https://doi.org/10.1039/c6ta04680k>
- Kumar, D., Meenan, B. J., Mutreja, I., D’Sa, R., & Dixon, D. (2012). Controlling the size and size distribution of gold nanoparticles: A design of experiment study. *International Journal of Nanoscience*, 11(2), 1–7. <https://doi.org/10.1142/S0219581X12500238>
- Kumari, J. M. K. W., Senadeera, G. K. R., Dissanayake, M. A. K. L., & Thotawatthage, C. A. (2017). Dependence of photovoltaic parameters on the size of cations adsorbed by TiO₂ photoanode in dye-sensitized solar cells. *Ionics*, 23(10), 2895–2900. <https://doi.org/10.1007/s11581-017-1995-z>
- Mcdonald, S. A., Konstantatos, G., Zhang, S., Cyr, P. W., Klem, E. J. D., Levina, L., & Sargent, E.



- H. (2005). Solution-processed PbS quantum dot infrared photodetectors and photovoltaics. *Nature Materials*, 4(2), 138–142. <https://doi.org/10.1038/nmat1299>
- Smith, J. G., Fauchaux, J. A., & Jain, P. K. (2015). Plasmon resonances for solar energy harvesting: A mechanistic outlook. *Nano Today*, 10(1), 67–80. <https://doi.org/10.1016/j.nantod.2014.12.004>

ACKNOWLEDGMENTS

This research was supported by the Accelerating Higher Education Expansion and Development (AHEAD) Operation (DOR 09) of the Ministry of Higher Education funded by the World Bank.